Mineralogical Magazine, August 2015, Vol. 79(4), pp. 857–876

Sm-Nd and Lu-Hf isotope and trace-element systematics of Mesoarchaean amphibolites, inner Ameralik fjord, southern West Greenland

Kristoffer Szilas[1,*], J. Elis Hoffmann[2,3,4], Christina Hansmeier[2], Julie A. Hollis[5,6], Carsten Münker[3], Sebastian Viehmann[7] and Haino U. Kasper[3]

[1] Stanford University, Department of Geological and Environmental Sciences, 450 Serra Mall, CA 94305, USA
[2] Steinmann Institut für Geologie, Mineralogie und Paläontologie, Abt. Endogene Prozesse, Rheinische Wilhelms-Universität Bonn, Poppelsdorfer Schloss, 53115 Bonn, Germany
[3] Universität zu Köln, Geologisch-Mineralogisches Institut, Albertus-Magnus-Platz, 50674 Köln, Germany
[4] Institut für Geologische Wissenschaften, Abt. Geochemie, Freie Universität Berlin, Malteserstrasse 74-100, 12249 Berlin, Germany
[5] Geological Survey of Denmark and Greenland, Øster Voldgade 10, 1350 Copenhagen K, Denmark
[6] Geological Survey of Western Australia, Mineral House, 100 Plain St, East Perth, WA 6000, Australia
[7] Jacobs University Bremen, Campus Ring 1, 28759 Bremen, Germany

[*Received 30 October 2014; Accepted 16 February 2015; Associate Editor: R. Mitchell*]

ABSTRACT

Fragmented supracrustal rocks are typical components of Archaean high-grade gneiss terranes, such as those in the North Atlantic Craton. Here we present the first major, trace element and Nd-Hf isotope data for amphibolites collected in the yet poorly studied southern inner Ameralik fjord region of southern West Greenland. In addition, new U-Pb zircon ages were obtained from the surrounding TTG gneisses.

Based on their trace-element patterns, two different groups of amphibolites can be distinguished. Following screening for post-magmatic alteration and outlying ε values, a reduced sample set defines a $^{147}Sm/^{143}Nd$ regression age of 3038 Ma ±310 Ma (MSWD = 9.2) and a $^{176}Lu/^{176}Hf$ regression age of 2867 ±160 Ma (MSWD = 5.5). Initial εNd_{2970Ma} values of the least-altered amphibolites range from 0.0 to +5.7 and initial εHf_{2970Ma} range from +0.7 to +10.4, indicating significant isotopic heterogeneity of their mantle sources with involvement of depleted domains as well as crustal sources.

Surprisingly, the amphibolites which are apparently most evolved and incompatible element-rich have the most depleted Hf-isotope compositions. This apparent paradox may be explained by the sampling of a local mantle source region with ancient previous melt depletion, which was re-enriched by a fluid component during subduction zone volcanism or alternatively by preferential melting of an ancient pyroxenite component in the mantle source of the enriched rocks.

Keywords: Nuuk region, Archaean, greenstone belt, supracrustal rocks, Hf isotope data.

Introduction

Remnants of supracrustal units and layered anorthosite intrusions are typical, but minor, components of Archaean high-grade gneiss terranes and include amphibolites, ultramafic

* E-mail: szilas@stanford.edu
DOI: 10.1180/minmag.2015.079.4.02

This paper is published as part of a special set in *Mineralogical Magazine*, Volume **79(4)**, 2015, arising out of the March 2014 NAC Conference on the North Atlantic Craton.

rocks and metasedimentary rocks (e.g. Condie, 1994; Hoffmann *et al.*, 2012; Mohan *et al.*, 2012). The major part of these terranes are up to 90% dominated by rocks classified broadly as the tonalite-trondhjemite-granodiorite (TTG) suite (e.g. Barker, 1979; Jahn *et al.*, 1981; Nutman *et al.*, 1996; Martin *et al.*, 1999; Moyen *et al.*, 2007; Hoffmann *et al.*, 2011*a*, Moyen and Martin, 2012). Depending on the degree of deformation, the supracrustal remnants and fragmented layered intrusions vary in size ranging from small metre-sized enclaves to km-scale supracrustal belts (e.g. Jackson, 1984; Martin, 1986; Nutman *et al.*, 1996, 2007; Polat *et al.*, 2007; Hoffmann *et al.*, 2012; Szilas *et al.*, 2012*a*,*b*). In many cases, the geological relationships between these fragmented rafts and the surrounding TTG gneisses are unclear due to ductile deformation and intrusion of later granites during post-magmatic tectonometamorphic events. Therefore, it is not clear if the supracrustal units can be linked to the TTG suites as potential protolith rocks that melted to produce the TTG (e.g. Adam *et al.*, 2012; Nagel *et al.*, 2012).

Zircon geochronology can help to unravel the relationships between different granitoid components. However, as zircon U-Pb geochronology is predominantly limited to felsic lithologies, the dating of supracrustal fragments is restricted to felsic and andesitic volcanic rocks and metasedimentary rocks that contain detrital zircon grains. Mafic and ultramafic rocks, however, typically crystallize at temperatures below that of magmatic zircon saturation (Watson and Harrison, 1983) and the majority of the zircons in these rock types crystallized during metamorphic events. Another way to date such metamorphosed mafic and ultramafic lithologies is with the application of whole-rock isochrons as it has been used successfully in previous studies (e.g. Ashwall *et al.*, 1983; Bhaskar Rao *et al.*, 1996) or direct dating of baddelyite, which is, however, not always present in mafic rocks. *In situ* Hf-isotope analyses of zircon from granitoids have become an increasingly popular tool for understanding crustal evolution and granitoid source materials (Belousova *et al.*, 2010; Dhuime *et al.*, 2012; Næraa *et al.*, 2012). However, granitoids are not directly mantle-derived, but can be the result of partial melting of pre-existing mafic crust (e.g. Rapp and Watson, 1995; Foley *et al.*, 2002; Clemens *et al.*, 2006) and thus it is critical to establish what the Hf isotope compositions are for regional supracrustal belts and mafic enclaves in order to test whether or not these inclusions in the gneisses in fact represent the source rocks for such granitoids.

In this study, we collected amphibolites from supracrustal fragments of a poorly studied area supposed to be dominated by Mesoarchaean gneisses and supracrustal remnants, inferred to be part of the Tasiusarsuaq terrane (e.g. Nutman and Friend, 2007) or the Tre Brødre terrane (Yi *et al.*, 2014), to investigate their age, their relationship to the surrounding TTG gneisses and to place constraints on their geodynamic setting. Therefore, we measured major and trace elements, as well as Lu-Hf and Sm-Nd isotope compositions of these rocks. In addition, two TTG samples were dated by U-Pb zircon geochronology to unravel the age relationship between the gneisses and supracrustal units in the area.

Geological background

The Nuuk region of southern West Greenland consists of several tectonostratigraphic terranes that were identified by extensive U-Pb zircon dating and geological mapping (e.g. Friend *et al.*, 1988, McGregor *et al.*, 1991, Nutman *et al.*, 2004; Nutman and Friend, 2007). These terranes are exposed in crustal blocks (Windley and Garde, 2009) and range in age from ~>3880 Ma to ~2800 Ma including the Eoarchaean Færringehavn and Isukasia terranes that make up the Itsaq gneiss complex (Nutman *et al.*, 1996; Hoffmann *et al.*, 2011*a*; Næraa *et al.*, 2012) and the Mesoarchaean Kapisillik, Tasiusarsuaq and Tre Brødre terranes (e.g. McGregor, 1991; Friend and Nutman, 2005). The samples collected for this study were collected from a largely unexplored area (Fig. 1), which has been grouped based on reconnaissance mapping and reconnaissance U-Pb zircon studies of the Geological Survey of Denmark and Greenland (GEUS) into the 2840–2920 Ma Tasiusarsuaq and the 2830–2800 Ma Tre Brødre terranes (Hollis, 2005). Friend and Nutman (2005) proposed naming this particular region as the Kapisilik terrane. However, Dziggel *et al.* (2014) showed that the previous terrane model for the Nuuk region needs to be revised and the crustal blocks could instead be viewed as paired metamorphic belts within the same accretionary complex. Here the Ameralik area is included as part of the Tasiusarsuaq terrane, because the supracrustal belts and anorthosite complexes in this crustal domain are indistinguishable from

https://doi.org/10.1180/minmag.2015.079.4.02 Published online by Cambridge University Press

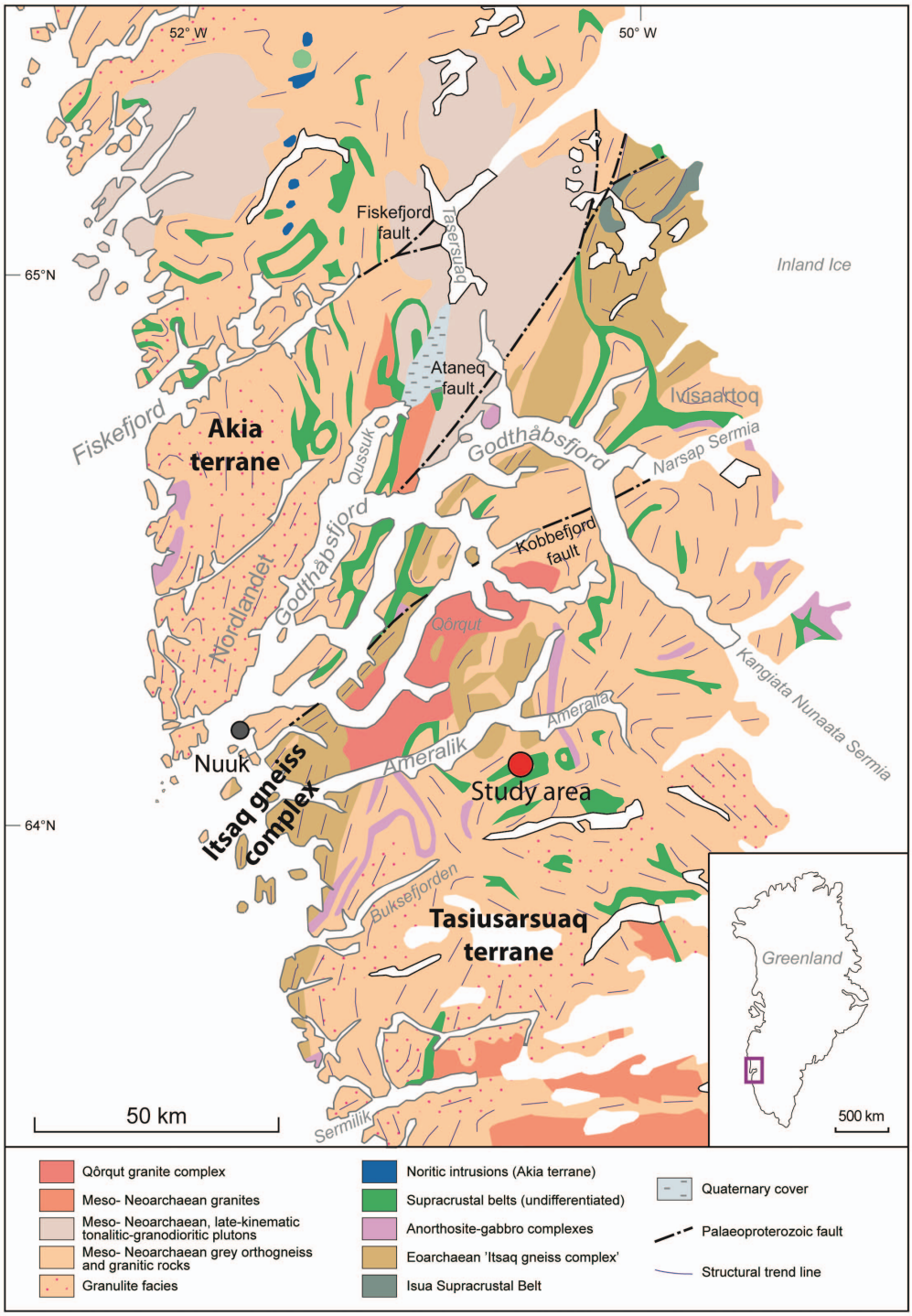

FIG. 1. Geological map of the Nuuk region, showing the study area outlined by the red dot. The map is based on work by the Geological Survey of Denmark and Greenland (GEUS).

https://doi.org/10.1180/minmag.2015.079.4.02 Published online by Cambridge University Press

those in the Fiskenæsset region as we will show below.

The area was mapped in 1978 by helicopter reconnaissance (Walton, 1976) and further mapping was carried out during the sampling work for this present study in 2005 (Rehnströhm, 2011). The area is dominated by compositionally layered tonalitic and granodioritic gneisses, up to hundreds of metre sized supracrustal remnants (amphibolites and ultramafic rocks), metasedimentary successions (garnet-mica schists, sillimanite- and cordierite-bearing schists, quartzites) and remnants of layered anorthosite complexes that are sheared and boudinaged into the adjacent TTG gneisses (Rehnström, 2011). The TTG orthogneisses (quartz-feldspar-biotite ± hornblende) in this region appear to have experienced a complicated history of deformation and *in situ* partial melting, as is typical for the adjacent Eoarchaean crust of the Itsaq gneiss complex. Several generations of late granites and pegmatites cut all the other rock units. The Tasiusarsuaq terrane is affected dominantly by amphibolite facies metamorphism, but granulite facies and retrogressed granulite facies metamorphism (Nutman and Friend, 2007; Schumacher *et al.*, 2011) as well as retrograde greenschist facies overprinted rocks were also found (Næraa and Scherstén, 2008). The area of this study was found to be dominated by amphibolite facies metamorphism. In the neighbouring area ~2 km to the southeast, retrogressed granulite facies rocks were discovered during reconnaissance mapping in 2005 and 2007. The protolith ages were dated to 2850 Ma and the metamorphic zircon grains yield ages of 2720 Ma (Hoffmann *et al.*, 2011*a*; Næraa *et al.*, 2012). Other supracrustal belts from the Tasiusarsuaq terrane south of the study area are better preserved, yielding primary intrusive relationships, primary structures and textures (gabbros, pillow basalts) and preserved compositional layering and volcaniclastic rocks (Szilas *et al.*, 2011, 2012*a*, 2012*b*, Keulen *et al.*, 2014). The 2970 Ma Naajat Kuuat layered anorthosite intrusion is located ~30 km to the east (Hoffmann *et al.*, 2012; Svahnberg, 2012), and layers of this mafic intrusion might be folded and migmatized to form the rocks of the area studied, as rare anorthosite and leucogabbro bands and inclusions are found within the gneisses. The Fiskenæsset anorthosite complex, also exposed within the Tasiusarsuaq terrane and with a similar age as the Naajat Kuuat Complex, is exposed ~100 km to the south and is much better preserved than the rocks studied here. Arc andesites, probably formed at a continental margin subduction zone, are also present in nearly all supracrustal belts (e.g. Garde, 2007; Szilas *et al.*, 2012*a*, 2013*a*), however, they have not been observed in the area studied here. This fits with structural data suggesting that accretionary processes were responsible for the formation of the Archaean crust of the North Atlantic (e.g. Windley and Garde, 2009; Kisters *et al.*, 2012; Dziggel *et al.*, 2014).

Sampling and petrography

Samples for this study were collected from the least altered amphibolite and ultramafic remnants within the TTG gneisses from the southern central Ameralik fjord region (Fig. 1). Nevertheless on closer inspection by thin-section petrography, two samples (496411 and 496418) were clearly altered, showing quartz veins, strong chloritization and strong overgrowth of the amphibole by biotite (Fig. 2). This higher degree of alteration compared to the other samples is also evident from their trace-element compositions (see section on major and trace elements below).

The amphibolite samples contain dominantly hornblende and plagioclase and occasionally preserve a gabbroic texture. In most samples, biotite is present, replacing the hornblende and some samples contain small quartz veins. Occasionally garnet was found in the amphibolites. Accessory phases include ilmenite, apatite and zircon. The ultramafic rocks contain olivine, green amphibole, plagioclase, pyroxenes and oxides.

Analytical techniques

Around 1–2 kg of each sample was cleaned from obvious alteration using a diamond coated rock saw, crushed with a jaw crusher and then powdered using an agate mill. Major-element compositions were obtained on Li-tetraborate glass disks by XRF using a Philips PW-1480 spectrometer at the Universität Bonn. For trace-element analyses, 100–150 mg of each sample powder were digested at 120ºC on a hot plate and subsequently placed for three days in Parr® bombs in an HF-HNO_3 acid mixture, following the analytical procedure described in Hoffmann *et al.* (2011*a*). Trace-element compositions were analysed by inductively-coupled mass spectrometry (ICP-MS) using a Perkin Elmer instrument

https://doi.org/10.1180/minmag.2015.079.4.02 Published online by Cambridge University Press

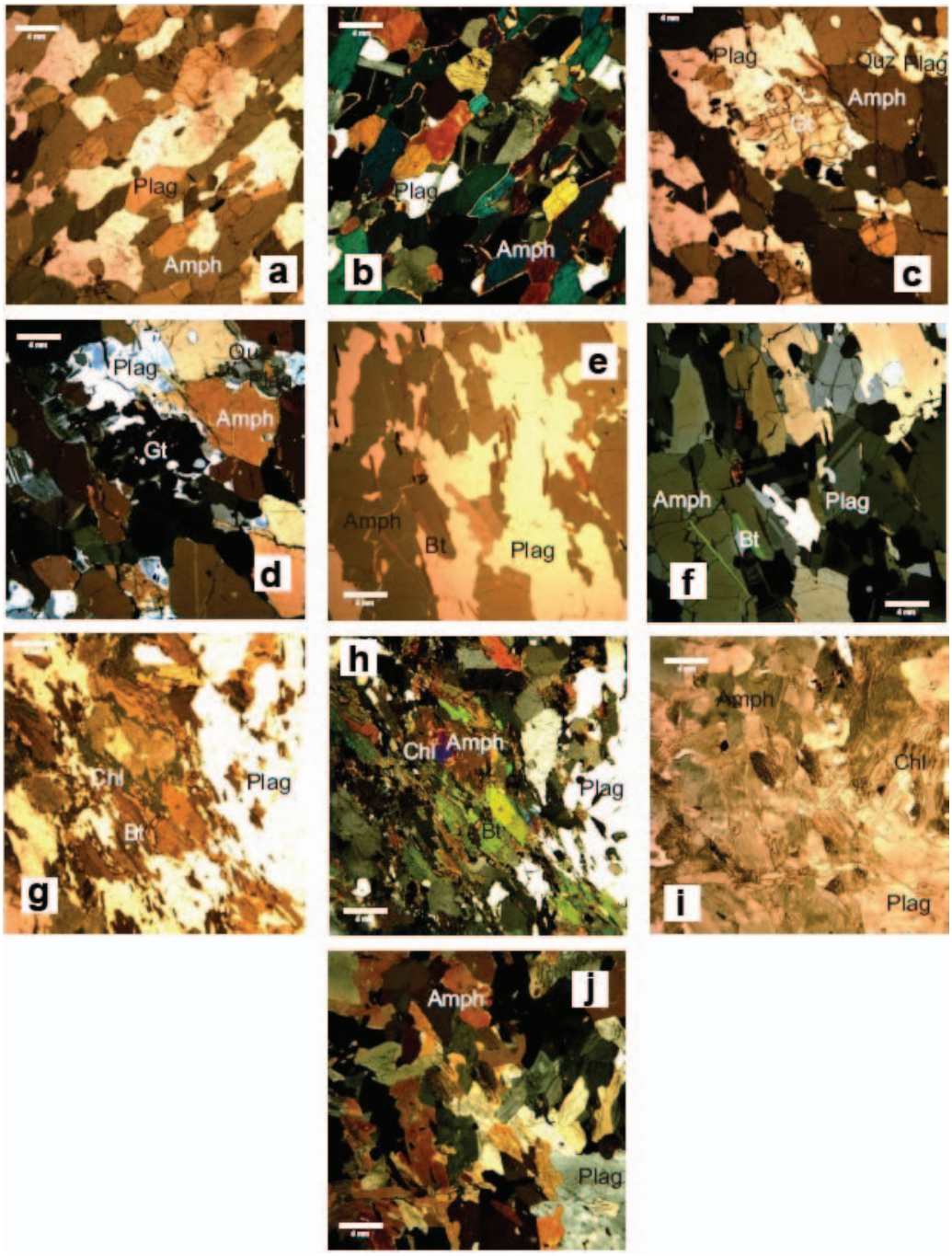

FIG. 2. Photomicrographs illustrating petrographic characteristics of the Ameralik amphibolite. (*a*, *b*) Sample 496415, typical amphibolite with plagioclase and amphibole; (*c*, *d*) 496410, garnet-amphibolite with amphibole, plagioclase, garnet and opaque phases; (*e*, *f*) 4996437: amphibolite with plagioclase and amphibole, which reacts to biotite at the grain boundaries; (*g*–*j*) 496411 and 496418, altered amphibolites where amphibole and plagioclase are altered to chlorite and biotite.

https://doi.org/10.1180/minmag.2015.079.4.02 Published online by Cambridge University Press

at the Universität zu Köln. The 2σ errors of the concentrations of the majority of elements were <10%, except for Pb which was considerably larger. Measurements of international standard reference materials BHVO-2 and BIR-1 are listed in Table 1 (which has been deposited with the Principal Editor of *Mineralogical Magazine* and is available from www.minersoc.org/pages/e_journals/dep_mat_mm.html) together with the results of sample analyses. The U-Pb age determination of the zircons by LA-ICP-MS followed the method described in detail by Frei and Gerdes (2009).

For the Lu-Hf and Sm-Nd isotope analyses, splits of 100–150 mg of sample powder were digested in a HF-HNO_3-$HClO_4$ acid mixture, first on the hot plate and subsequently in Parr® bombs following the digestion procedure of Hoffmann *et al.* (2011*b*). Prior to digestion the powders were spiked with ^{176}Lu-^{180}Hf and ^{149}Sm-^{150}Nd tracers. Lutetium and Hf were separated using the one column chemistry of Münker *et al.* (2001). Samarium and Nd were retrieved from the leftover matrix using conventional cation-exchange resin and Ln-spec resin following the method of Pin and Zaldegui (1997). Lutetium, Hf, Sm, Nd concentrations and ^{176}Lu/^{176}Hf and ^{147}Sm/^{143}Nd ratios of the S-Ameralik samples were determined by isotope dilution techniques using a Neptune MC-ICP-MS at the joint Cologne-Bonn isotope lab following the protocols of Münker *et al.* (2001) and Weyer *et al.* (2002). For Hf isotope compositions all measurements were corrected to a ^{179}Hf/^{177}Hf of 0.7325 applying the exponential law. The long term reproducibility of the ^{176}Hf/^{177}Hf for the Münster AMES solution that is isotopically indistinguishable from JMC-475 is ±40 ppm (2σ), measured ^{176}Hf/^{177}Hf values were 0.282159 ± 42 (n = 8) and 0.282163 ± 33 (n = 12), respectively. All data are given relative to a ^{176}Hf/^{176}Hf of 0.282160 for Münster AMES. The external reproducibility for ^{176}Lu/^{177}Hf is 0.2% as determined from multiple measurements of natural samples. Mass fractionation correction for ^{143}Nd/^{144}Nd was carried out relative to a ^{146}Nd/^{144}Nd of 0.7219 using the exponential law. Values obtained for a 20 ppb La Jolla standard were ^{143}Nd/^{144}Nd of 0.511773 ± 51 (n = 2) and 0.511798 ± 34 (n = 2), all data are given relative to a ^{143}Nd/^{144}Nd of 0.511859 for La Jolla. La Jolla measurements were complemented by measurements of several in-house standards calibrated against La Jolla. The long term reproducibility for the ^{143}Nd/^{144}Nd of La Jolla is ±40 ppm (2s) and 0.2% for ^{147}Sm/^{144}Nd. Procedural blanks were <12 pg for Lu, <50 pg for Hf, <50 pg for Sm and <50 pg for Nd.

Results

Major and trace elements

The sample set from the Ameralik fjord region can be broadly divided into two groups which consist of: (1) amphibolites and (2) ultramafic rocks. Only 2 samples out of the 16 analysed samples are clearly altered (samples 496411 and 496418) and therefore, were excluded from the description of the two main groups in the following sections. Major- and trace-element analyses are presented in Table 1 (deposited at www.minersoc.org/pages/e_journals/dep_mat_mm.html). The data reported has been normalized on a volatile-free basis and is referred to in the discussion of the data throughout this paper.

The amphibolites (n = 11) are characterized by 48.2–51.0 wt.% SiO_2, 4.5–9.1 wt.% MgO, 0.56–2.96 wt.% TiO_2, 12.6–15.3 wt.% Al_2O_3, 8.78–12.3 wt.% CaO, 1.89–3.07 wt.% Na_2O, 0.25–1.75 wt.% K_2O (Fig. 3). The loss on ignition (LOI) of the amphibolites varies from 0.1 to 1.5 wt.%, with one sample having a negative LOI of −0.3wt.%. The trace-element compositions of the amphibolites are variable with $(La/Yb)_{CN}$ ranging from 0.73 to 3.71 and Eu/Eu* from 0.81 to 0.93. Chromium and Ni contents are also variable ranging from 1.4 to 355 and 29 to 129 ppm, respectively.

Two sub-groups can be identified among the amphibolites based on their trace-element abundances, namely a high rare-earth elements (*REE*) group and a low-*REE* group (Figs 3 and 4). The trace-element patterns of these two amphibolite groups are essentially sub-parallel, although there are minor differences, such as $(La/Yb)_{CN}$ of 1.4–3.7 and 0.7–1.6, respectively. However, the main differences within the Ameralik fjord amphibolites are dependent on the absolute element concentrations and not on their trace-element behaviour. Within the two groups one significant difference is primitive mantle-normalized negative Sr-anomalies of the high-*REE* group, compared to positive Sr anomalies of the low-*REE* group (Fig. 4). These two amphibolite groups are also distinct in terms of their major-element compositions, with the high-*REE* group having less MgO and Al_2O_3, but greater TiO_2 and Fe_2O_3 (Fig. 3), thus being Fe-tholeiitic, whereas

https://doi.org/10.1180/minmag.2015.079.4.02 Published online by Cambridge University Press

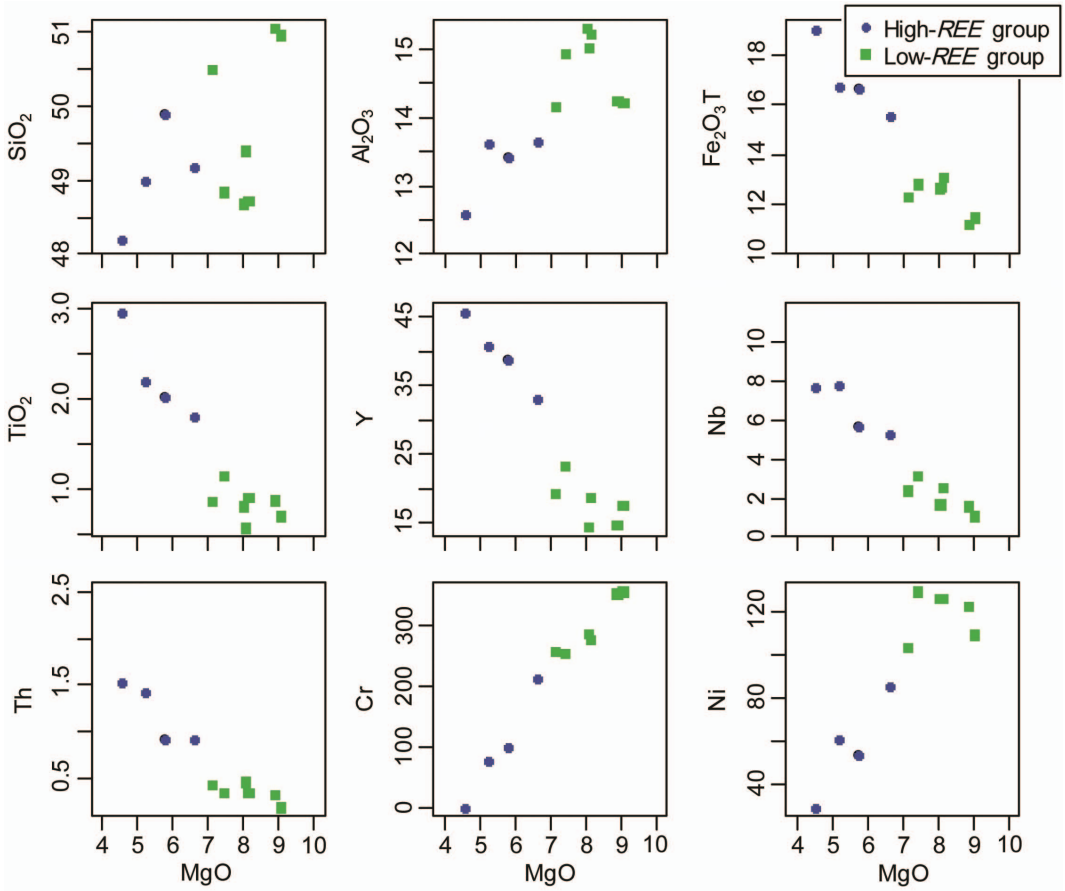

FIG. 3. Selected major and trace elements as a function of MgO contents for the high- and low-*REE* amphibolite groups. Note the correlations against MgO, which are typical trends in evolving magmas, where incompatible elements are enriched as Mg-bearing minerals crystallize. Oxides are in wt.% and trace elements are in ppm.

the low-*REE* group is Mg-tholeiitic. As we show in the section on ^{147}Sm-^{143}Nd and ^{176}Lu-^{176}Hf isotope data below, these two groups also have important differences in their Hf-isotope compositions.

The ultramafic rocks (n = 3) are characterized by having 14.8–30.2 wt.% MgO, 3.1–6.5 wt.% Al_2O_3, 510–2665 ppm Cr, 558–1399 ppm Ni and generally low trace-element compositions, with the exception of sample 496402, which shows elevated trace-element abundances. They have variable normative mineralogy, but are dominated by clinopyroxene (up to 35%), orthopyroxene (up to 35%), plagioclase (up to 20%) and one sample has normative olivine (29%).

The two altered samples display distinct compositional characteristics compared to the amphibolites and ultramafic rocks. Sample 496411 has elevated SiO_2, K_2O and incompatible element abundances relative to the low-*REE* amphibolite group, which it otherwise shares major-element features with. It appears to have a crustal overprint with elevated trace-element composition in combination with distinctly negative Ti-, Nb- and Ta-anomalies. Sample 496418 is characterized by the largest CaO contents (19.5 wt.%) of the sample set and also the largest LOI at 3.8 wt.%. This, in combination with strongly positive Sr and Eu anomalies and *LREE* enrichment, indicates significant carbonation of this sample. The elevated Cr and Ni content of this sample at 1957 and 761 ppm, respectively, suggest that the precursor rock was ultramafic.

https://doi.org/10.1180/minmag.2015.079.4.02 Published online by Cambridge University Press

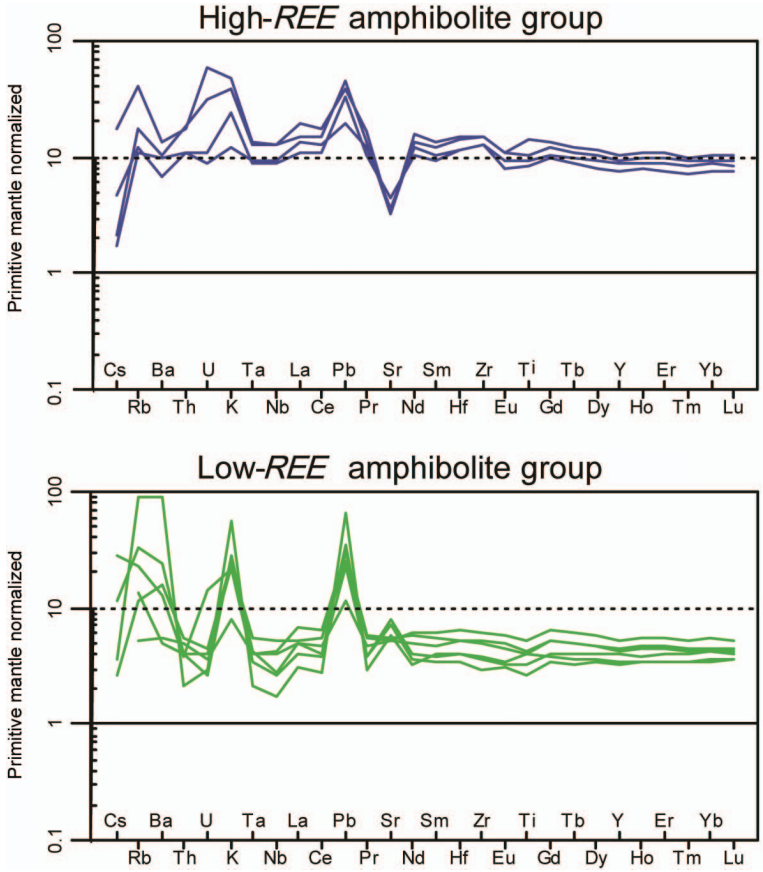

FIG. 4. Primitive mantle-normalized trace-element diagrams for the least altered low- and high-*REE* amphibolite groups. Note the corresponding Sr anomalies. Primitive mantle values from Palme and O'Neill (2003).

^{147}Sm-^{143}Nd and ^{176}Lu-^{176}Hf isotope data

Although the Sm-Nd and Lu-Hf isotope compositions of our samples plot along an errorchron line they do not provide precise age constraints (Figs 5*a* and 6*a*) We have calculated Nd- and Hf-episilon (ε) values at 2970 Ma according to the precise age for the Fiskenæsset complex (Polat *et al.*, 2010) and 3075 Ma according to the age for the Ivisaartoq supracrustal belt (Polat *et al.*, 2007). These two ages represent major volcanic events in this region, which are thus also potential estimates of the magmatic age of the Ameralik rocks presented in this study. Given that these rocks are associated spatially with anorthosite sheets and that the main orthogneisses have an age that is similar to those of the Tasiuarsuaq terrane (see the section on U-Pb zircon geochronology), we prefer the age of 2970 Ma for the Ameralik amphibolites. The ^{147}Sm/^{144}Nd ratio varies from 0.095610 to 0.228960 and initial εNd values at 2970 Ma are between −0.1 and +5.7 and εNd at 3075 Ma are from +0.2 to +5.7. The ^{176}Lu/^{177}Hf ratios vary from 0.008150 to 0.046050 and initial εHf values at 2970 Ma for all of the samples are between −9.9 and +10.4 (Fig. 7) and at 3075 Ma −9.4 to +11.2. This range of ε values is similar to the results of other studies from supracrustal belts in the Tasiusarsuaq terrane of similar age (e.g. Scherstén *et al.*, 2008, Ordonez-Calderon *et al.*, 2008, 2009, 2011; Szilas *et al.*, 2012*a*, 2013*a*,*b*; Hoffmann *et al.*, 2012). After screening out the obviously altered samples and the ones that could represent cumulates the data form tighter isochrons, as seen in Figs 5*b* and 6*b* with ages of 3038 ±310 Ma (MSWD = 9.2) and 2867 ±160 Ma (MSWD = 5.5), respectively. The Sm-Nd and Lu-Hf isotope

https://doi.org/10.1180/minmag.2015.079.4.02 Published online by Cambridge University Press

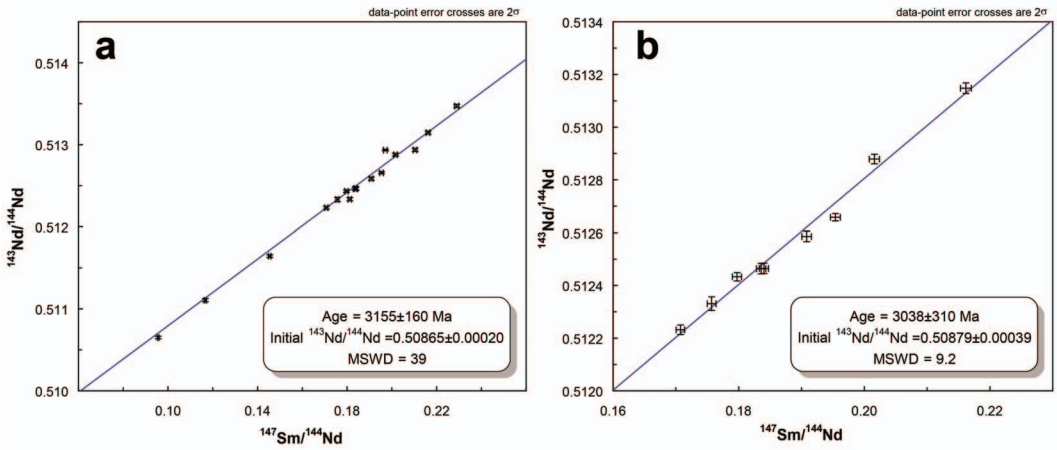

FIG. 5. Sm-Nd isochron diagram for all samples (*a*) and for selected samples within a tight εNd_{2970Ma} range between +0.9 and +2.8 (*b*). NB. the low-*REE* amphibolite group with elevated εNd has not been measured for its trace-element contents, but is assumed to have similar abundances to the rest of the samples in this group. MSWD: Mean square weighted deviation.

data are presented in Table 2 (deposited with the Principal Editor of *Mineralogical Magazine* and available at www.minersoc.org/pages/e_journals/dep_mat_mm.html).

U-Pb zircon geochronology

Uranium-lead (U-Pb) zircon geochronology was performed on zircons separated from a homogeneous tonalite sample (sample 496408) and a migmatitic tonalite (sample 496417) collected within the sampled area. Examples of the zircons that were recovered from these rocks are shown in Fig. 8. Additional images of the zircon grains can be found in Appendix A which has been deposited with the Principal Editor of *Mineralogical Magazine* and is available from www.minersoc.org/pages/e_journals/dep_mat_mm.html. The U-Pb isotope data are presented in Table 3 (available at www.minersoc.org/pages/e_journals/dep_mat_mm.html) and Figs 9 and 10.

Sample 496408 yields a $^{206}Pb/^{207}Pb$ age of 2867 ±11 Ma, when excluding the two obvious younger and older grains. A metamorphic age of 2741 ±17 Ma is hinted by a single analysis of a homogeneous zircon rim, in agreement with other

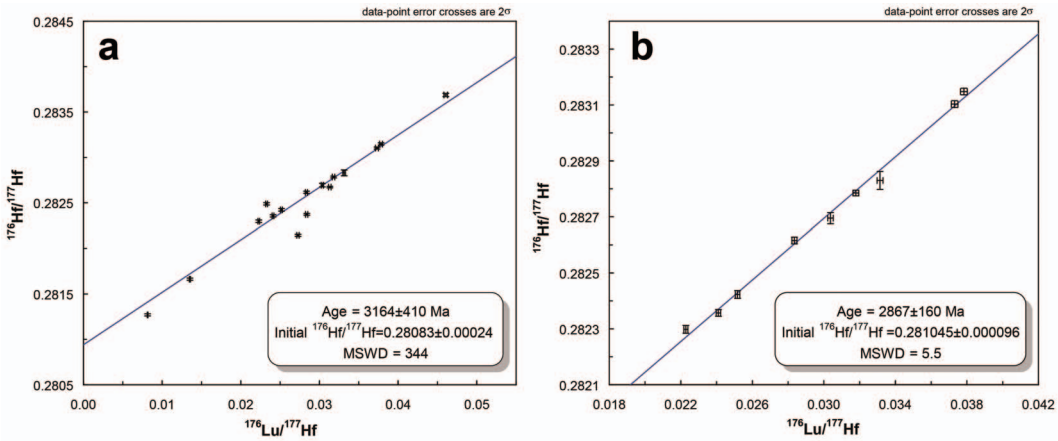

FIG. 6. Lu-Hf isochron diagram for (*a*) all samples and (*b*) for selected samples within a tight εHf_{2970Ma} range between +2.5 and +5.6.

https://doi.org/10.1180/minmag.2015.079.4.02 Published online by Cambridge University Press

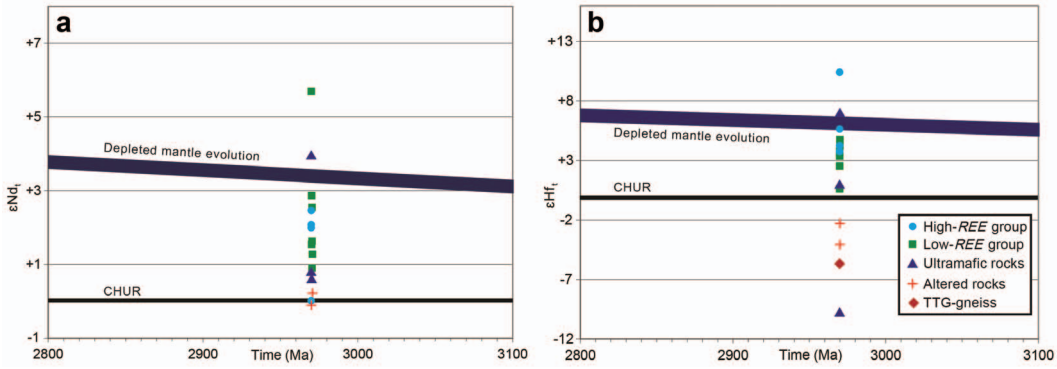

FIG. 7. Diagrams of εNd *vs*. time (*a*) and εHf *vs*. time (*b*) with the samples plotted at 2970 Ma. We have plotted the εHf composition of TTG gneiss sample 468645 with a magmatic age of 3255 Ma (Næraa *et al.*, 2012) recalculated to its composition at 2970 Ma to give an example of older regional crust, which could represent a potential contamination source. Note that several samples have isotope compositions that plot significantly above the depleted mantle evolution line indicating highly depleted sources or assimilation of components with ancient depletion.

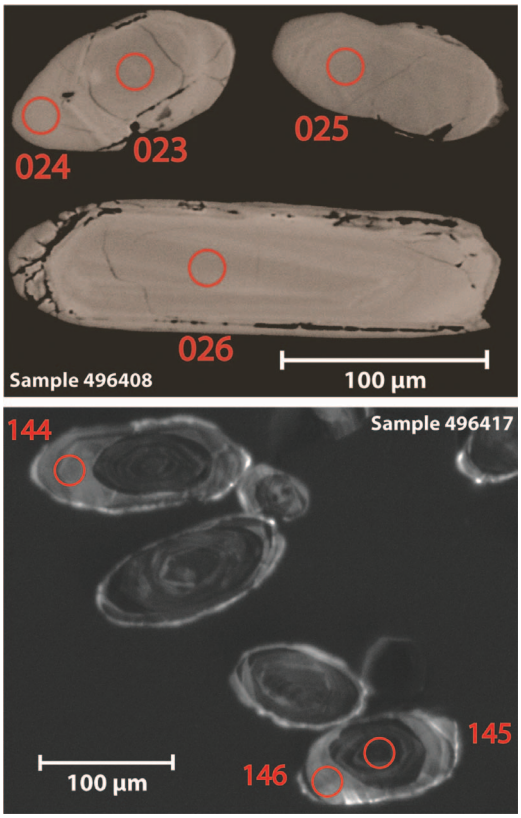

FIG. 8. Examples of zircon grains in samples 496408 and 496417 showing back-scattered electron and cathodoluminescence images, respectively. Note the visible difference between the oscillatory zoned cores and the homogeneous rims. See Appendix A (deposited) for additional zircon images.

TTG samples from the Tasiusarsuaq terrane (Friend and Nutman, 2005; Næraa and Scherstén., 2008; Szilas *et al.*, 2013*a*).

Sample 496417 has an Eoarchaean $^{207}Pb/^{206}Pb$ age of ~3613 Ma (90% of the analyses based on peak unmixing in Isoplot/EX 3.71). Three younger grains are from zircon rims and thus probably represent metamorphic zircon growth.

Discussion

Influence of alteration

All the samples were screened carefully for alteration. Thin sections were inspected to identify samples with carbonate alteration and quartz veining. Photomicrographs of typical amphibolite samples are shown in Fig. 2; Figs 2*a–f* represent well preserved samples and Figs 2*g–j* show altered samples being chloritized and yielding a strong overgrowth of amphibole by biotite. The best preserved samples were further screened using their major- and trace-element composition following the procedures described by Polat *et al.* (2002) and Polat and Hofmann (2003). As mentioned in the results, two samples were clearly altered, namely sample 496411, which has elevated SiO_2, K_2O and incompatible element abundances relative to the low-*REE* amphibolite group, and sample 496418 with elevated CaO, LOI, Sr, Eu and *LREE*. Although we cannot entirely rule out that some samples may have experienced some degree of post-magmatic disturbance, the remaining samples display consistent correlations between immobile

https://doi.org/10.1180/minmag.2015.079.4.02 Published online by Cambridge University Press

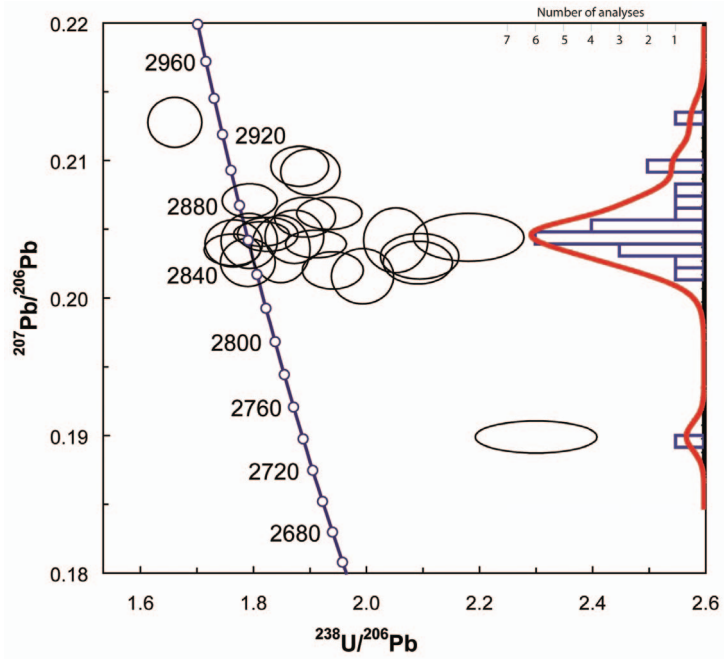

FIG. 9. Tera-Wasserburg concordia diagram for the zircon U-Pb isotope data from sample 496408. A probability density diagram (red curve) and the number of analyses are shown on the right side. The magmatic ages of this sample is calculated as 2867 ±11 Ma (see the section on U-Pb zircon geochronology).

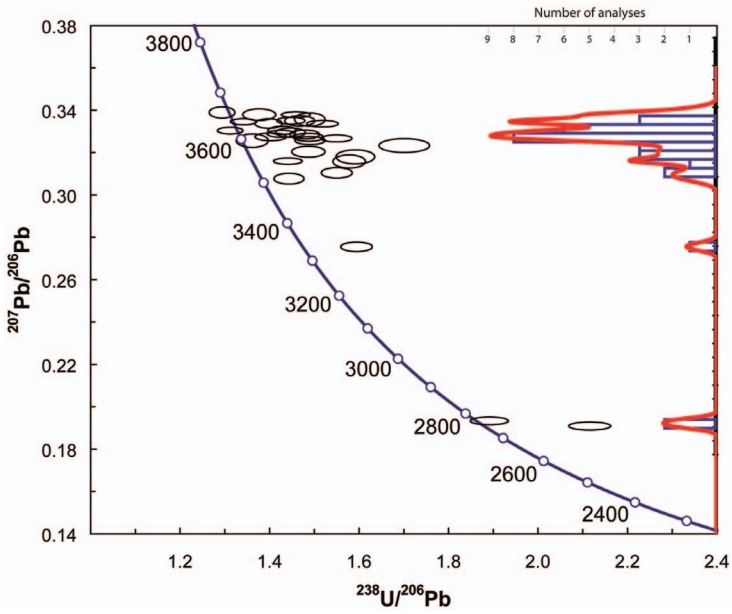

FIG. 10. Tera-Wasserburg concordia diagram for the zircon U-Pb isotope data from sample 496417. A probability density diagram (red curve) and the number of analyses are shown on the right side. This sample has a main peak ~3613 Ma (see the section on U-Pb zircon geochronology).

https://doi.org/10.1180/minmag.2015.079.4.02 Published online by Cambridge University Press

elements and broadly follow trends that are seemingly consistent with fractional crystallization processes (Fig. 3).

Major- and trace-element characteristics

The apparently continuous major- and trace-element trends of the Ameralik amphibolites, suggest that the high- and low-*REE* groups could be potentially related to fractional crystallization processes (Fig. 3). This is also indicated by their corresponding positive- and negative Sr-anomalies (Fig. 4). The major- and trace-element compositions of the low-*REE* group of amphibolites are similar to regional mafic tholeiitic rocks in the supracrustal belts of southwest Greenland (e.g. Polat *et al.*, 2007; Szilas *et al.*, 2011, 2013*b*). The high-*REE* group on the other hand, does not plot along the typical olivine-controlled fractional crystallization series, typical for such mafic assemblages. Although the high-*REE* group of amphibolites have some similarities in major-element compositions with calc-alkaline leucoamphibolites from the Ravns Storø supracrustal belt south of the Fiskenæsset complex (Szilas *et al.*, 2012*a*), there are also some important differences, such as significantly higher Fe_2O_{3T} and TiO_2 in the former rocks. Additionally, the high-*REE* amphibolites from the Ameralik area have distinctly higher abundances of *HREE* and hence flatter trace-element patterns than crustally contaminated rocks such as the leucoamphibolites from Ravns Storø. In detail, the geochemical variation of the amphibolites is not compatible with crustal assimilation or mixing processes during eruption. Although they fall on crystal fractionation trends, it would require unrealistically large percentages of fractionation (Fig. 11), which is not consistent with the major-element compositions (Fig. 3). Fractional crystallization of plagioclase would be able to explain the smaller CaO and Al_2O_3 content of the high-*REE* group, but not the overall larger trace-element abundances. As we show in the section on ^{147}Sm-^{143}Nd and ^{176}Lu-^{176}Hf isotope systematics below, fractional crystallization processes are also not consistent with the observed

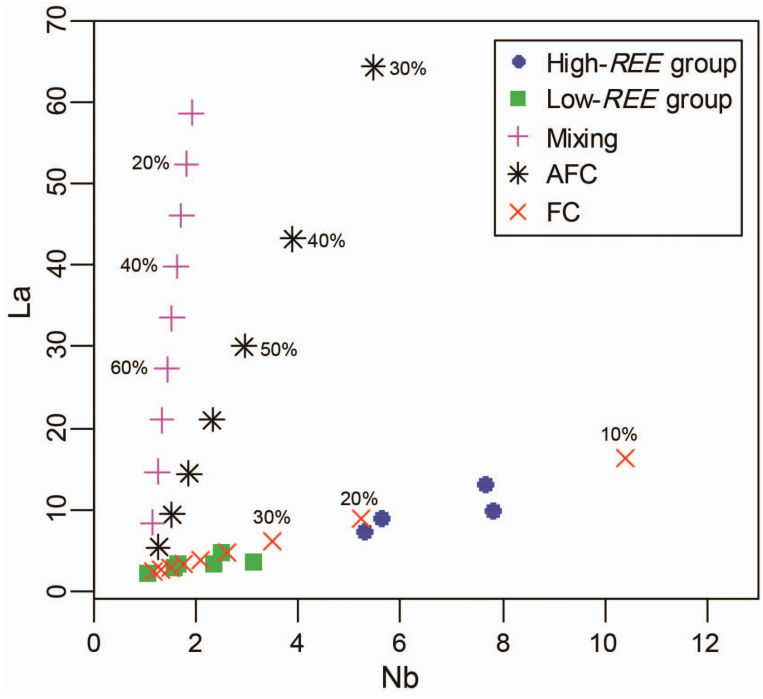

FIG. 11. Modelling of fractional crystallization (FC), assimilation-fractional crystallization (AFC) and mixing in a La *vs*. Nb diagram. Sample 496409 is used as the starting composition and TTG gneiss sample 496408 is used as a proxy for the crustal contaminant. An *r* factor of 0.3 is used and the melt fraction remaining is showed in 10% steps.

https://doi.org/10.1180/minmag.2015.079.4.02 Published online by Cambridge University Press

differences in the isotope compositions of the high- and low-*REE* amphibolites.

We have compared the three ultramafic samples analysed with data from the nearby Naajat Kuuat Complex, which show obvious olivine-dominated fractional crystallization trends (Hoffmann *et al.*, 2012). Szilas *et al.* (2012*b*) reported geochemical data for serpentinites in the Tasiusarsuaq terrane that were proposed to represent ultramafic lavas. However, detailed geochemical studies on similar Archaean ultramafic rocks in other parts of southwest Greenland, concluded that olivine+spinel cumulates mixed with up to 50% of the liquids, from which these minerals fractionated to form the ultramafic protoliths for abundant serpentinites in these volcanic associations (Szilas *et al.*, 2014, 2015). Thus, it appears that the geochemical variation in such ultramafic rocks probably represents formation of olivine-rich cumulates, which may have trapped inter-cumulus liquids or accumulated plagioclase. This would also explain the observed combination of depleted major-element compositions, while still having incompatible trace-element patterns that are broadly parallel with the associated volcanic sequence, in the Ameralik fjord supracrustal rocks. In the case of the Ameralik ultramafic rocks the normative mineralogy suggests that the protoliths of some of these rocks may have been pyroxenites.

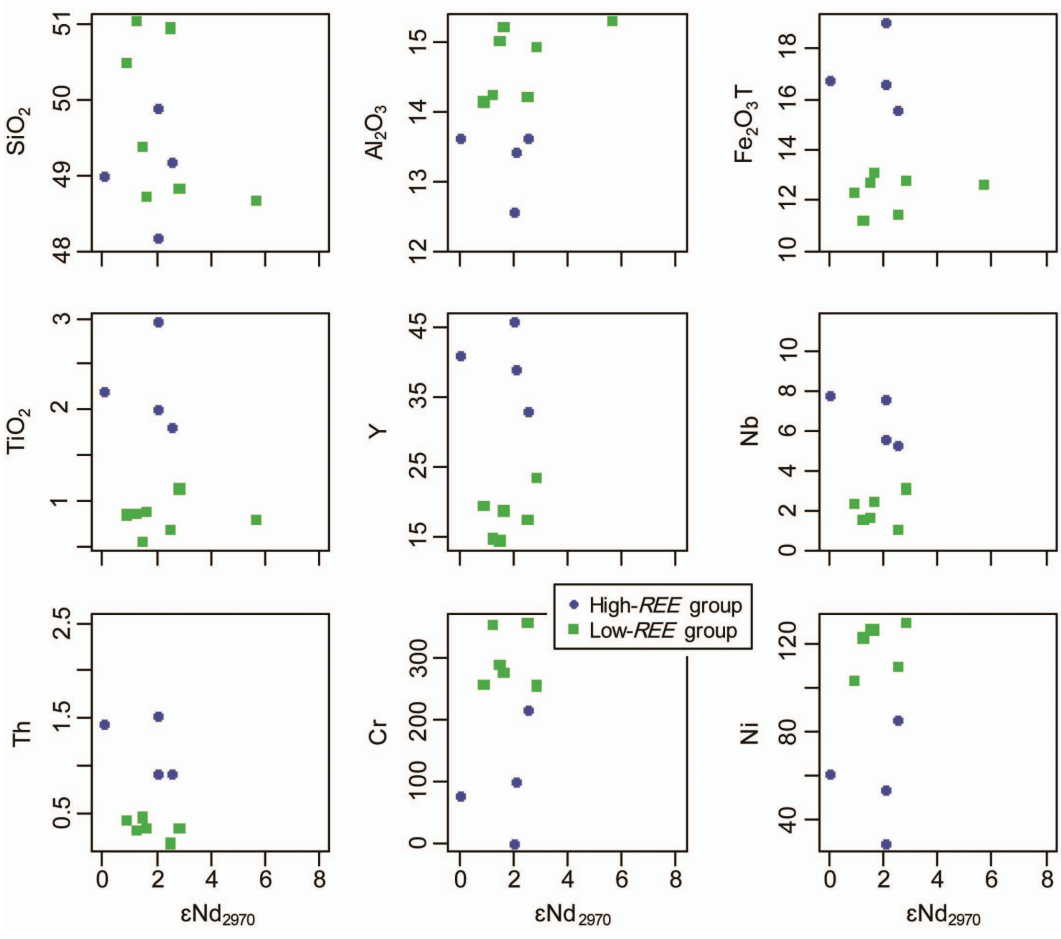

FIG. 12. Selected major and trace elements as a function of εNd_{2970Ma} for the high- and low-*REE* amphibolite groups. Note that on average the apparently most evolved rocks are the most radiogenic. However, this effect is more obvious for the Hf-isotope compositions (see Fig. 13).

https://doi.org/10.1180/minmag.2015.079.4.02 Published online by Cambridge University Press

^{147}Sm-^{143}Nd and ^{176}Lu-^{176}Hf isotope systematics

The Hf-Nd isotope compositions in combination with major- and trace-element systematics can provide constraints on the mantle sources of mantle-derived rocks. For the S-Ameralik fjord samples note that the apparently most evolved mafic rocks (low MgO, high *LREE*, Zr, TiO_2 etc.) are also the most radiogenic (Figs 12 and 13). The paradox that the apparently most evolved rocks with elevated incompatible element abundances (high-*REE* group) have the most radiogenic Hf isotope compositions (εHf_{2970Ma} up to +10.4) can only be explained by different source compositions for the high- and low-*REE* amphibolite groups (Fig. 7*b*). We have plotted the TTG gneiss sample 468645 of Næraa *et al.* (2012) with an age of 3255 Ma as the representative of older regional crust. This sample had εHf_{2970Ma} of −5.6 and thus a crust of this composition could potentially account for the isotopic overprint of the Ameralik samples (except for sample 496401, which is even less radiogenic) if it interacted with the mantle-derived melts. However, crustal contamination cannot explain the Hf isotope compositions of the two most radiogenic samples. Surprisingly, the Nd isotope compositions (Fig. 7*a*) show some overlap between the high- and low-*REE* groups, sample 499301 (low-*REE*). This observation points to the decoupling of Nd and Hf isotope systematics. For example, the low-*REE* sample 499301 has elevated initial εNd at a low initial εHf value and the high-*REE* sample

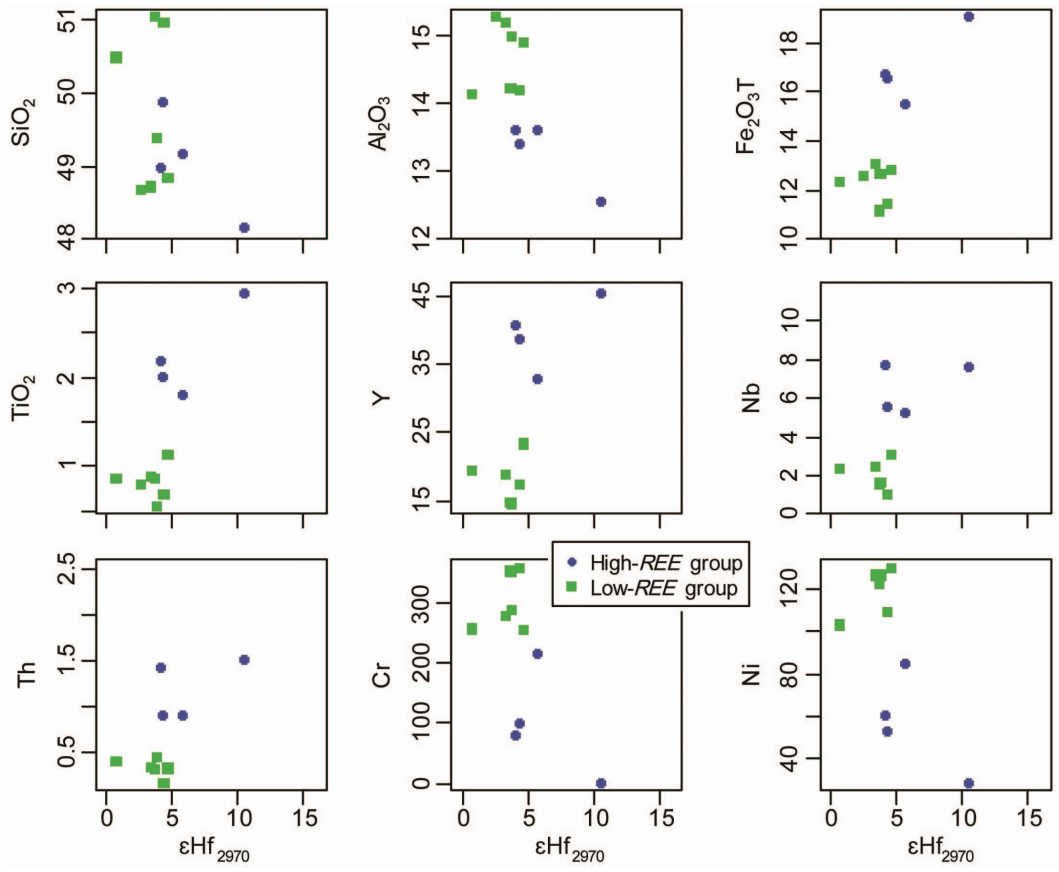

FIG. 13. Selected major and trace elements as a function of εHf_{2970Ma} for the high- and low-*REE* amphibolite groups. Note that the apparently most evolved rocks are the most radiogenic. Initial εHf were calculated using the ^{176}Lu decay constant of Scherer *et al.* (2001) and Söderlund *et al.* (2004) and the CHUR (chondritic uniform reservoir) values of Bouvier *et al.* (2008).

https://doi.org/10.1180/minmag.2015.079.4.02 Published online by Cambridge University Press

496426 has elevated initial Hf at relatively low initial εNd. This argues against late-stage crustal assimilation and suggests that there was primary mantle-source heterogeneity perhaps with the involvement of ancient highly depleted domains based on the initial Nd- and Hf-isotope compositions, which are significantly more radiogenic than the depleted mantle at 2970 Ma. The lack of correlations between crustal contamination indices and the isotope compositions within the two amphibolite groups (Fig. 14), points to a variable isotope composition of their mantle source and thus perhaps variable degrees of slab melt or sediment overprinting prior to partial melting.

U-Pb age constraints on the orthogneisses

The zircon geochronology of sample 496408 (~2867 Ma), reveals that that TTG gneisses in the Ameralik area have ages that are typical of the Tasiusarsuaq terrane. However, the smaller outcrop sampled by 496417 (~3613 Ma) shows that Eoarchaean Itsaq gneisses are also exposed in this area. The small 150 m × 300 m sized outcrop of Eoarchaean crust either represents a mega-xenolith within the Tasiusarsuaq terrane or it is structurally intercalated with the Mesoarchaean rocks of the area and possibly the basement to the younger gneisses. Alternatively, the Mesoarchaean rocks have been juxtaposed upon the Eoarchaean crust and the small-scale outcrop is just exposed because of complex folding. The overall structure of the area is very complex and is not currently understood. This outcrop of Eoarchaean crust that we have dated is located several km south of the supposed terrane boundary of Nutman and Friend (2007) and thus further fieldwork is needed in order to establish the relationships between the different terranes. Nevertheless, the age of ~3613 Ma is one of the youngest TTG ages measured so far within the Itsaq gneiss complex.

Geodynamic implications

The supracrustal belts along the western margin of southern West Greenland yield similar ages of

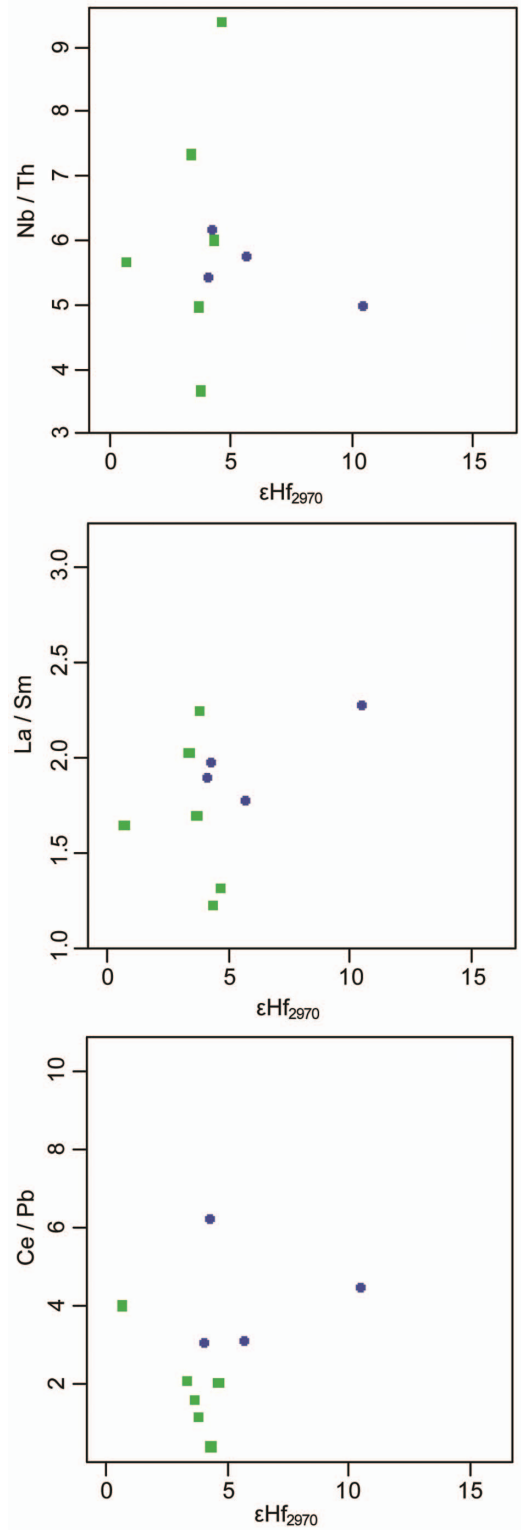

FIG. 14. Trace-element ratios *vs*. εHf_{2970Ma} diagram. Symbols are the same as in Fig. 3. The two groups of amphibolites do not appear to be related by crustal contamination, but could potentially represent derivation from different mantle source compositions.

https://doi.org/10.1180/minmag.2015.079.4.02 Published online by Cambridge University Press

~2985–2970 Ma. Specifically, these include mafic assemblages within the Tasiusarsuaq terrane, such as the Fiskenæsset complex (Polat *et al.*, 2010), the Ravns Storø and Bjørnesund supracrustal belts (Szilas *et al.*, 2012*a*), the Grædefjord supracrustal belt (Szilas *et al.*, 2013*a*) and the Naajat Kuuat Complex (Hoffmann *et al.*, 2012). All of these mafic rocks predate the local TTG orthogneisses, however, even older gneisses have also been reported (Næraa, 2011). The isotope signature of crustal assimilation has been also described by some studies (Friend *et al.*, 2008; Hoffmann *et al.*, 2012; Szilas *et al.*, 2012*a*, 2013*a*; Souders *et al.*, 2013) supporting evidence for a continental margin geodynamic setting. From the geochemistry of the supracrustal fragments of the southern inner Ameralik area presented in this work, there is also a tendency towards an unradiogenic isotope composition for both the Sm-Nd as well as for the Lu-Hf isotope system. However, as shown in the discussion on major- and trace-element characteristics, the detailed trace-element variation points towards a source overprint or magma chamber assimilation processes, rather than crustal assimilation during eruption. This was also concluded for the above-mentioned rock associations (e.g. Szilas *et al.*, 2012*a*, 2013*a*).

Overall, the combined isotope and trace-element systematics for rocks in the Tasiusarsuaq terrane are compatible with a subduction zone geodynamic setting, with both juvenile contributions, as well as with influence from a pre-existing continental margin. This is seen in Fig. 15, where some of the high-*REE* amphibolites clearly plot within the field of Isua boninites (Hoffmann *et al.*, 2010), which are inferred to have been derived from a mantle source that experienced ancient melt extraction in combination with later refertilization (Polat *et al.*, 2002). The gneisses of the Tasiusarsuaq and the Akia terrane are also probably the product of interaction with older continental crust as reflected by their variable but near to chondritic Hf and Nd initial isotope compositions and the presence of rare cases of inherited zircon grains (Friend *et al.*, 2008; Hoffmann *et al.*, 2011*a*; Næraa *et al.*, 2012), which also supports a continental margin setting.

In the present study we find evidence for highly depleted mantle domains, as also reported for anorthosites by Polat *et al.* (2010) and Szilas *et al.* (2012*a*), as well as for early Archaean boninite-like rocks from Isua (Hoffmann *et al.*, 2010). This observation is also consistent with a subduction zone setting, where previously depleted mantle domains are refertilized by melt and/or fluids and attests to complex accretionary processes during the Mesoarchaean.

Conclusions

The following conclusions can be drawn from the data presented in this study for Mesoarchaean amphibolites from the southern inner Ameralik fjord:

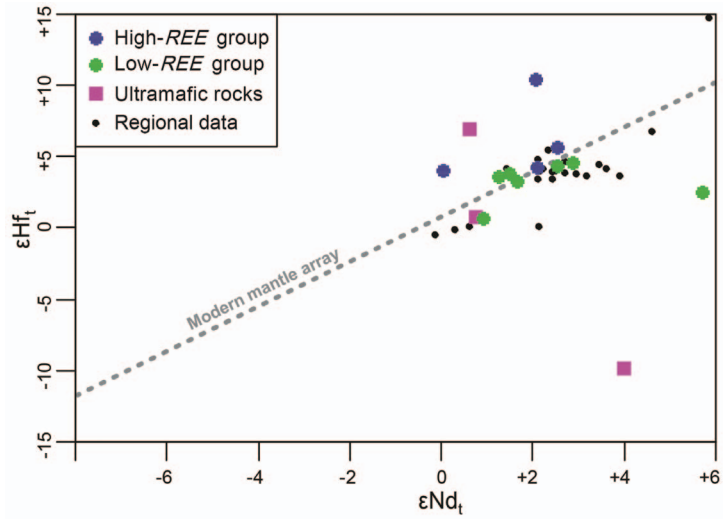

FIG. 15. Diagram of εHf_{2970Ma} *vs.* εNd_{2970Ma} showing the modern day mantle array (stippled line) and the fields of Eoarchaean rocks from SW Greenland. Regional data from Szilas *et al.* (2012*a*, 2013*a*)

https://doi.org/10.1180/minmag.2015.079.4.02 Published online by Cambridge University Press

(1) The geochemical compositions of these amphibolites are comparable to those of other supracrustal rocks within the Tasiusarsuaq terrane. Major- and trace-element compositions are in agreement with an arc-related setting. Crustal assimilation alone cannot explain the differences in incompatible trace-element patterns between the high- and low-*REE* groups of amphibolites.

(2) The Nd- and Hf-isotope compositions are consistent with a volcanic age of ~2970 Ma for the amphibolites presented in this study, which also appears to be the main magmatic event in the Tasiusarsuaq terrane. The isotope data points to involvement of a depleted mantle source, which was overprinted by slightly less radiogenic material (crustal, slab and/or sediment melts?). At the same time there is also evidence for a more radiogenic component with εNd_{2970Ma} up to +5.7 and εHf_{2970Ma} up to +10.4. This depleted source could potentially be explained by mantle domains that experienced ancient melt depletion and were subsequently refertilized during subduction zone processes or alternatively by preferential melting of enriched pyroxenite components.

(3) A typical TTG sample from the region is 2867 Ma, similar to the ages obtained for other Tasiusarsuaq TTG gneisses. However, Eoarchaean components (~3613 Ma) are also present in the area.

Acknowledgements

The authors thank Graham Pearson for a review that improved this paper and Roger Mitchell for editorial handling of the manuscript. This study is based on data reported in two unpublished Masters theses, at the University of Bonn by C.H. and the University of Münster by J.E.H. The current research was founded by the DFG (German Research Foundation) grant MU 1406/8, HO 4694/1-1 and by GEUS (Geological Survey of Denmark and Greenland). R. Hoffbauer is thanked for help with the XRF analyses. The authors are grateful to Adam A. Garde, Henrik Svahnberg, Sandra Piazolo and Daniel Herwartz for discussions in the field and help during fieldwork.

References

Adam, J., Rushmer, T., O'Neil, J. and Francis, D. (2012) Hadean greenstones from the Nuvvuagittuq fold belt and the origin of the Earth's early continental crust. *Geology*, **40**, 363–366.

Ashwal, L.D., Morrison, D.A., Phinney, W.C. and Wood, J. (1983) Origin of Archean anorthosites: evidence from the Bad Vermilion Lake complex, Ontario. *Contributions to Mineralogy and Petrology*, **82**, 259–273.

Barker, F., Arth, J.G. and Millard, H.T. (1979) Archaean trondhjemites of the southwestern Big Horn Mountains, Wyoming: a preliminary report. Pp. 401–414 in: *Trondhjemites, Dacites and Related Rocks* (F. Barker, editor). Elsevier, Amsterdam.

Belousova, E.A., Kostitsyn, Y.A., Griffin, W.L., Begg, G.C., O'Reilly, S.Y. and Pearson, N.J. (2010) The growth of the continental crust: constraints from zircon Hf-isotope data. *Lithos*, **119**, 457–466.

Bhaskar Rao, Y.J., Chetty, T.R.K., Janardhan, A.S. and Gopalan, K. (1996) Sm-Nd and Rb-Sr ages and P-T history of the Archean Sittampundi and Bhavani layered meta-anorthosite complexes in Cauvery shear zone, South India: Evidence for neoproterozoic reworking of archean crust. *Contributions to Mineralogy and Petrology*, **125**, 237–250.

Bouvier, A., Vervoort, J.D. and Patchett, P.J. (2008) The Lu–Hf and Sm–Nd isotopic composition of CHUR: constraints from unequillibrated chondrites and applications for the bulk composition of terrestrial planets. *Earth and Planetary Science Letters*, **273**, 48–57.

Clemens, J.D., Yearron, L.M. and Stevens, G. (2006) Barberton (South Africa) TTG magmas: Geochemical and experimental constraints on source-rock petrology, pressure of formation and tectonic setting. *Precambrian Research*, **151**, 53–78.

Condie, K.C. (editor) (1994) *Archean Crustal Evolution*. Developments in Precambrian Geology **11**. Elsevier, Amsterdam, 528 pp.

Dhuime, B., Hawkesworth, C.J., Cawood, P.A. and Storey, C.D., (2012) A change in the geodynamics of continental growth 3 billion years ago. *Science*, **335**, 1334–1336.

Dziggel, A., Diener, J.F.A., Kolb, J. and Kokfelt, T.F. (2014) Metamorphic record of accretionary processes during the Neoarchaean: The Nuuk region, southern West Greenland. *Precambrian Research*, **242**, 22–38.

Foley, S.F., Tiepolo, M. and Vannucci, R. (2002) Growth of early continental crust controlled by melting of amphibolite in subduction zones. *Nature*, **417**, 837–840.

Frei, D. and Gerdes, A. (2009) Accurate and precise in-situ zircon U-Pb age dating with high spatial resolution and high sample throughput by automated LA-SF-ICP-MS. *Chemical Geology*, **261**, 261–270.

Friend, C.R.L. and Nutman, A.P. (2005) New pieces to the Archaean terrane jigsaw puzzle in the Nuuk

https://doi.org/10.1180/minmag.2015.079.4.02 Published online by Cambridge University Press

region, southern West Greenland: steps in transforming a simple insight into a complex regional tectonothermal model. *Journal of the Geological Society*, **162**, 147–162.

Friend, C.R.L., Nutman, A.P. and McGregor, V.R. (1988) Late Archean terrane accretion in the Godthab region, southern West Greenland. *Nature*, **335**, 535–538.

Friend, C.R.L., Nutman, A.P., Baadsgaard, H. and Duke, M.J.M. (2008) The whole rock Sm–Nd 'age' for the 2825 Ma Ikkattoq gneisses (Greenland) is 800 Ma too young: Insights into Archaean TTG petrogenesis. *Chemical Geology*, **261**, 62–76.

Garde, A.A. (2007) A mid-Archean island arc complex in the eastern Akia terrane, Godthåbsfjord, southern West Greenland. *Journal of the Geological Society of London*, **164**, 565–579.

Hoffmann, J.E., Münker, C., Polat, A., König, S., Mezger, K. and Rosing, M.T. (2010) Highly depleted Hadean mantle reservoirs in the sources of early Archean arc-like rocks, Isua supracrustal belt, southern West Greenland. *Geochimica et Cosmochimica Acta*, **74**, 7236–7260.

Hoffmann, J.E., Münker, C., Næraa, T., Rosing, M.T., Garbe-Schönberg, D. and Svahnberg, H. (2011*a*) Mechanisms of Archean crust formation inferred from high-precision HFS systematics in TTGs. *Geochimica et Cosmochimica Acta*, **75**, 4157–4178.

Hoffmann, J.E., Münker, C., Polat, A., Rosing, M.T. and Schulz, T. (2011*b*) Origin of decoupled Hf–Nd isotope compositions in Eoarchean rocks from southern West Greenland. *Geochimica et Cosmochimica Acta*, **75**, 6610–6628.

Hoffmann, J.E., Svahnberg, H., Piazolo, S., Scherstén, A. and Muenker, C. (2012) The geodynamic evolution of Mesoarchean anorthosite complexes inferred from the Naajat Kuuat Complex, southern West Greenland. *Precambrian Research*, **196**, 149–170.

Hollis, J.A. (editor) (2005) *Greenstone belts in the central Godthåbsfjord region, southern West Greenland*. Danmarks og Grønlands Geologiske Undersøgelse rapport 2005/42. GEUS, Copenhagen, 215 pp.

Jackson, M.P.A. (1984) Archaean structural styles in the Ancient Gneiss Complex of Swaziland, southern Africa. Pp. 1–18 in: *Precambrian Tectonics Illustrated* (A. Kroner and R. Greiling, editors). Schweizerbart, Stuttgart, Germany.

Jahn, B., Glikson, A.Y., Peucat, J.-J. and Hickman, A.H. (1981) REE geochemistry and isotopic data of Archaean silicic volcanics and granitoids from the Pilbara block, western Australia: implications for early crustal evolution. *Geochimica et Cosmochimica Acta*, **45**, 1633–1652.

Keulen, N., Schumacher, J.C., Næraa, T., Kokfelt, T.F., Scherstén, A., Szilas, K., van Hinsberg, V.J., Schlatter, D.M. and Windley, B.F. (2014) Meso- and Neoarchaean geological history of the Bjørnesund and Ravns Storø Supracrustal Belts, southern West Greenland: Settings for gold enrichment and corundum formation. *Precambrian Research*, **254**, 36–58.

Kisters, A.F., van Hinsberg, V.J. and Szilas, K. (2012) Geology of an Archaean accretionary complex—The structural record of burial and return flow in the Tartoq Group of South West Greenland. *Precambrian Research*, **220**, 107–122.

Martin, H. (1986) Effect of steeper Archean geothermal gradient on geochemistry of subduction-zone magmas. *Geology*, **14**, 753–756.

Martin, H. (1999) Adakitic magmas: modern analogues of Archaean granitoids. *Lithos*, **46**, 411–429.

McGregor, V.R., Friend, C.R.L. and Nutman, A.P. (1991) The late Archaean mobile belt through Godthabsfjord, southern West Greenland: a continent-continent collision zone? *Bulletin of the Geological Society of Denmark*, **39**, 179–197.

Mohan, M.R., Satyarayanan, M., Santosh, M., Sylvester, P.J., Tubrett, M. and Lam, R. (2012) Neoarchean suprasubduction zone arc magmatism in southern India: Geochemistry, zircon U-Pb geochronology and Hf isotopes of the Sittampundi Anothosite Complex. *Gondwana Research*, **23**, 539–557.

Moyen, J.F. and Martin, H. (2012) Forty years of TTG research. Lithos, **148**, 312–336.

Moyen, J.F., Stevens, G., Kisters, A.F.M. and Belcher, R.W. (2007) TTG plutons of the Barberton granitoid-greenstone terrain, South Africa. Pp. 607–667 in: *Earth's Oldest Rocks* (M.J. van Kranendonk, R.H. Smithies and V.C. Bennett (editors). Developments in Precambrian Geology (K.C. Condie, Series editor), **vol. 15**. Elsevier B.V., Amsterdam.

Münker, C., Weyer, S., Scherer, E. and Mezger, K. (2001) Separation of high field strength elements (Nb, Ta, Zr, Hf): and Lu from rock samples for MC-ICPMS measurements. *Geochememistry Geophysics Geosystems 2 (G3)*, **2(12)**, doi:10.1029/2001GC000183.

Næraa, T. and Scherstén, A. (2008) New zircon ages from the Tasiusarsuaq terrane, southern West Greenland. *Geological Survey of Denmark and Greenland Bulletin*, **15**, 73–76.

Næraa, T. (2011) *Zircon U/Pb, Hf and O isotope systematics from the Archaean Basement in the Nuuk region, southern West Greenland: Constrains on the early evolution of the continental crust*. Doctoral dissertation, Københavns Universitet, Copenhagen.

Næraa, T., Scherstén, A., Rosing, M.T., Kemp, A.I.S., Hoffmann, J.E., Kokfelt, T.F. and Whitehouse, M.J. (2012) Hafnium isotope evidence for a transition in the dynamics of continental growth 3.2 Gyr ago.

https://doi.org/10.1180/minmag.2015.079.4.02 Published online by Cambridge University Press

Nature, **485(7400)**, 627–630.

Nagel, T.J., Hoffmann, J.E. and Münker, C. (2012) Generation of Eoarchean tonalite–trondhjemite–granodiorites series from thickened mafic arc crust. *Geology*, **40**, 375–378.

Nutman, A.P. and Friend, C.R.L. (2007) Adjacent terranes with ca. 2715 and 2650 Ma high-pressure metamorphic assemblages in the Nuuk region of the North Atlantic Craton, southern West Greenland: Complexities of Neoarchean collisional orogeny. *Precambrian Research*, **155**, 159–203.

Nutman, A.P., McGregor, V.R., Friend, C.R.L., Bennett, V.C. and Kinny, P.D., 1996. The Itsaq Gneiss Complex of southern West Greenland: the world's most extensive record of early crustal evolution (3900–3600 Ma). *Precambrian Research*, **78**, 1–39.

Nutman, A.P., Friend, C.R.L., Barker, S.L.L. and McGregor, V.R. (2004) Inventory and assess- ment of PalaeoArchean gneiss terrains and detrital zircons in southern West Greenland. *Precambrian Research*, **135**, 281–314.

Ordónez-Calderon, J.C., Polat, A., Fryer, B.J., Gagnon, J.E., Raith, J.G. and Appel, P.W.U. (2008) Evidence for HFSE and REE mobility during calc-silicate metasomatism, Mesoarchean (c.3075 Ma) Ivisaartoq greenstone belt, southern West Greenland. *Precambrian Research*, **161**, 317–340.

Ordónez-Calderon, J.C., Polat, A., Fryer, B.J., Appel, P.W.U., van Gool, J.A.M., Dilek, Y. and Gagnon, J.E. (2009) Geochemistry and geodynamic origin of the Mesoarchean Ujarassuit and Ivisaartoq greenstone belts, SW Greenland. *Lithos*, **113**, 133–157.

Ordónez-Calderon, J.C., Polat, A., Fryer, B. and Gagnon, J.E. (2011) Field and geochemical characteristics of Mesoarchean to Neoarchean volcanic rocks in the Storø green- stone belt, SW Greenland: evidence for accretion of intra-oceanic volcanic arcs. *Precambrian Research*, **184**, 24–42.

Palme, H. and O'Neill, H.C. (2003) Compositional estimates of mantle composition. Pp. 1–38 in: *The Mantle and Core*, **vol. 2** (Carlson, R.W., editor). Elsevier-Pergamon, Oxford, UK.

Pin, C. and Zalduegui, J.S. (1997) Sequential separation of light rare-earth elements, thorium and uranium by miniaturized extraction chromatography: application to isotopic analyses of silicate rocks. *Analytica Chimica Acta*, **339**, 79–89.

Polat, A. and Hofmann, A.W. (2003) Alteration and geochemical patterns in the 3.7–3.8 Ga Isua greenstone belt, West Greenland. *Precambrian Research*, **126**, 197–218.

Polat, A., Hofmann, A.W. and Rosing, M.T. (2002) Boninite-like volcanic rocks in the 3.7–3.8 Ga Isua greenstone belt, West Greenland: geochemical evidence for intra-oceanic subduction zone processes in the early Earth. *Chemical Geology*, **184**, 231–254.

Polat, A., Appel, P.W., Frei, R., Pan, Y., Dilek, Y., Ordóñez-Calderón, J.C. and Raith, J.G. (2007) Field and geochemical characteristics of the Mesoarchean (~ 3075 Ma) Ivisaartoq greenstone belt, southern West Greenland: Evidence for seafloor hydrothermal alteration in supra-subduction oceanic crust. *Gondwana Research*, **11**, 69–91.

Polat, A., Frei, R., Scherstén, A. and Appel, P.W. (2010) New age (ca. 2970 Ma), mantle source composition and geodynamic constraints on the Archean Fiskenæsset anorthosite complex, SW Greenland. *Chemical Geology*, **277**, 1–20.

Rapp, R.P. and Watson, E.B. (1995) Dehydration melting of metabasalt at 8-32 kbar: Implications for continental growth and crust-mantle recycling. *Journal of Petrology*, **36**, 891–931.

Rehnström, E.F. 2011. *Geological Map of Greenland 1:100000, Kapisillit 64 V.2 Syd*. Geological Survey of Denmark and Greenland, Copenhagen.

Scherer, E., Münker, C. and Mezger, K. (2001) Calibration of the lutetium–hafnium clock. *Science*, **293**, 683–687.

Scherstén, A., Stendal, H. and Næraa, T. (2008) Geochemistry of greenstones in the Tasiusarsuaq terrane, southern West Greenland. *Geological Survey of Denmark and Greenland Bulletin*, **15**, 69–72.

Schumacher, J.C., van Hinsberg, V.J. and Keulen, N. (2011) *Metamorphism in supracrustal and ultramafic rocks in southern West Greenland and South-West Greenland 64.–61.5° N*. Danmarks og Grønlands Geologiske Undersøgelse Rapport 2011/06. GEUS, Copenhagen, 29 pp.

Söderlund, U., Patchett, P.J., Vervoort, J.D. and Isachsen, C.E. (2004). The 176 Lu decay constant determined by Lu–Hf and U–Pb isotope systematics of Precambrian mafic intrusions. *Earth and Planetary Science Letters*, **219**, 311–324.

Souders, A.K., Sylvester, P.J. and Myers, J.S. (2013) Mantle and crustal sources of Archean anorthosite: a combined *in-situ* study of Pb-Pb and Lu-Hf in zircon. *Contributions to Mineralogy and Petrology*, **165**, 1–24.

Svahnberg, H. (2012) *Deformation and chemical signatures of anorthosites – Examples from southern West Greenland and south-central Sweden*. Meddelanden fran Stockholms universitets Institution för geologiska vertenskaper No. 340. Doctoral Thesis, Stockholm University, Sweden.

Szilas, K., van Hinsberg, V.J., Kisters, A.F., Kokfelt, T.F., Scherstén, A. and Windley, B.F. (2011) Remnants of Mesoarchaean oceanic crust in the Tartoq Group, South-West Greenland. *Geological Survey of Denmark and Greenland Bulletin*, **23**, 57–60.

Szilas, K., Hoffmann, J.E., Scherstén, A., Rosing, M.T., Windley, B.F., Kokfelt, T.F. and Münker, C. (2012*a*)

https://doi.org/10.1180/minmag.2015.079.4.02 Published online by Cambridge University Press

Complex calc-alkaline volcanism recorded in Mesoarchaean supracrustal belts north of Frederikshåb Isblink, southern West Greenland: Implications for subduction zone processes in the early Earth. *Precambrian Research*, **208**, 90–123.

Szilas, K., Næraa, T., Scherstén, A., Stendal, H., Frei, R., van Hinsberg, V.J. and Rosing, M.T. (2012*b*) Origin of Mesoarchaean arc-related rocks with boninite/komatiite affinities from southern West Greenland. *Lithos*, **144**, 24–39.

Szilas, K., Hoffmann, J.E., Scherstén, A., Kokfelt, T.F. and Münker, C. (2013*a*) Archaean andesite petrogenesis: Insights from the Grædefjord Supracrustal Belt, southern West Greenland. *Precambrian Research*, **236**, 1–15.

Szilas, K., van Hinsberg, V.J., Kisters, A.F.M., Hoffmann, J.E., Windley, B.F., Kokfelt, T.F., Scherstén, A., Frei, R., Rosing, M.T. and Münker, C. (2013*b*) Remnants of arc-related Mesoarchaean oceanic crust in the Tartoq Group of SW Greenland. *Gondwana Research*, **23**, 436–451.

Szilas, K., van Hinsberg, V.J., Creaser, R.A. and Kisters, A.F.M (2014) The geochemical composition of serpentinites in the Mesoarchaean Tartoq Group, SW Greenland: Harzburgitic cumulates or melt-modified mantle? *Lithos*, **198**–**199**, 103–116.

Szilas, K., Kelemen, P.B. and Rosing, M.T. (2015) The petrogenesis of ultramafic rocks in the >3.7 Ga Isua supracrustal belt, southern West Greenland: Geochemical evidence for two distinct magmatic cumulate trends. *Gondwana Research*, **28**, 565–580.

Walton, B.J. (1976) *Geological Map 1:50000 64 V.2 37b*. Grønlands Geologiske Undersøgelse, Copenhagen.

Watson, E.B. and Harrison T.M. (1983) Zircon saturation revisited: temperature and composition effects in a variety of crustal magma types. *Earth and Planetary Science Letters*, **64**, 295–304.

Weyer, S., Münker, C., Rehkämper, M. and Mezger, K. (2002) Determination of ultra-low Nb, Ta, Zr and Hf concentrations and the chondritic Zr/Hf and Nb/Ta ratios by isotope dilution analyses with multiple collector ICP-MS. *Chemical Geology*, **187**, 295–313.

Windley, B.F. and Garde, A.A. (2009) Arc-generated blocks with crustal sections in the North Atlantic craton of West Greenland: Crustal growth in the Archaean with modern analogues. *Earth Science Reviews*, **93**, 1–30.

Yi, K., Bennett, V.C., Nutman, A.P. and Lee, S.R. (2014) Tracing Archaean terranes under Greenland's Icecap: U–Th–Pb–Hf isotopic study of zircons from melt-water rivers in the Isua area. *Precambrian Research*, **255**, 900–921.

https://doi.org/10.1180/minmag.2015.079.4.02 Published online by Cambridge University Press